Li *et al. Collagen and Leather* 2023, **4**(1):29
https://doi.org/10.1186/s42825-022-00105-3

Collagen and Leather

RESEARCH

Open Access

Polyphenol based hybrid nano-aggregates modified collagen fibers of biological valve leaflets to achieve enhanced mechanical, anticoagulation and anti-calcification properties

Shufen Li[1†], Shiying Lang[2†], Zhiqian Chen[3], Jingruo Chen[1], Weihua Zhuang[1], Yangrui Du[2], Yawen Yao[4], Gongyan Liu[2*] and Mao Chen[1,5,6*]

Abstract

Glutaraldehyde (Glut)-crosslinked porcine pericardium and bovine pericardium are mainly consisted of collagen and widely used for the preparation of heterogenous bioprosthetic heart valves (BHV), which play an important role in the replacement therapy of severe valvular heart disease, while their durability is limited by degeneration due to calcification, thrombus, endothelialization difficulty and prosthetic valve endocarditis. Herein, we develop a novel BHV, namely, TPly-BP, based on natural tannic acid and polylysine to improve the durability of Glut crosslinked bovine pericardium (Glut-BP). Impressively, tannic acid and polylysine could form nanoaggregates via multiple hydrogen bonds and covalent bonds, and the introduction of nanoaggregates not only improved the mechanical properties and collagen stability but also endowed TPly-BP with good biocompatibility and hemocompatibility. Compared to Glut-BP, TPly-BP showed significantly reduced cytotoxicity, improved endothelial cell adhesion, a low hemolysis ratio and obviously reduced platelet adhesion. Importantly, TPly-BP exhibited great antibacterial and in vivo anti-calcification ability, which was expected to improve the in vivo durability of BHVs. These results suggested that TPly-BP would be a potential candidate for BHV.

Keywords Tannic acid, Bioprosthetic heart valve, Antibacterial and anti-calcification

[†]Shufen Li and Shiying Lang contributed equally to this work

*Correspondence:
Gongyan Liu
lgy3506@scu.edu.cn
Mao Chen
chenmao@scu.edu.cn
Full list of author information is available at the end of the article

Graphical abstract

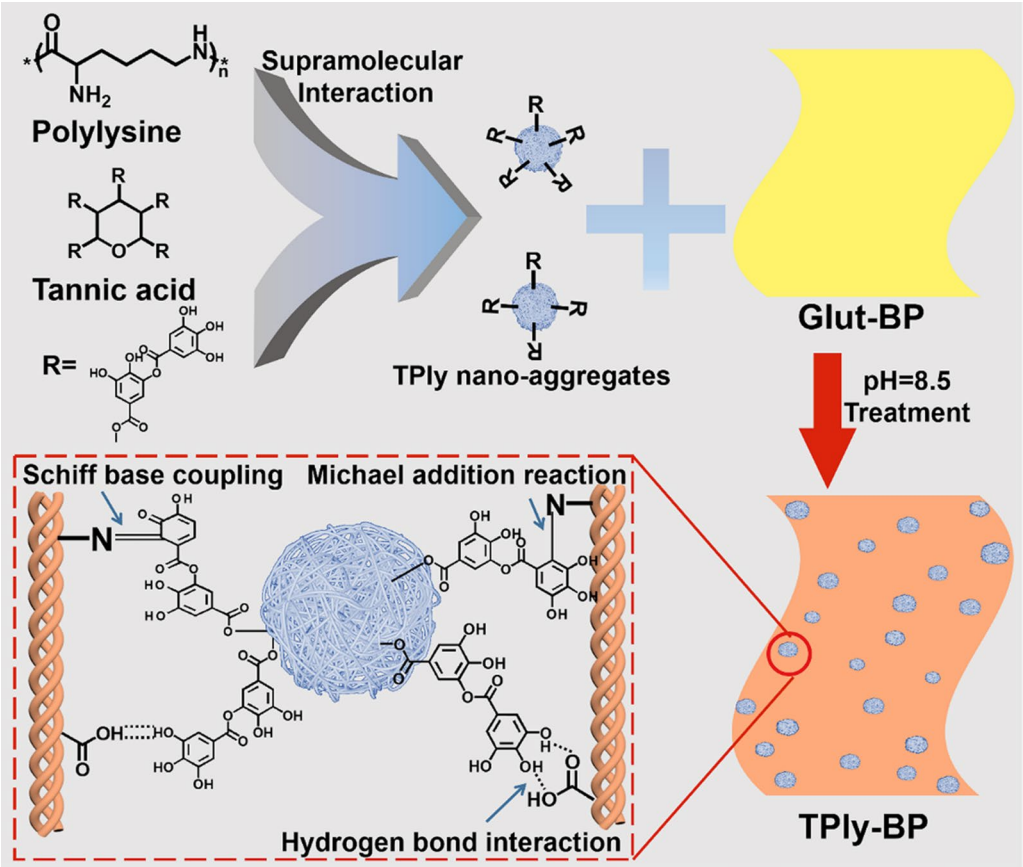

1 Introduction

Valvular heart disease (VHD) affects approximately 74 million people around the world, and it has been one of the greatest threats to human health attributed to the increase in the aging population, which would induce cardiac dysfunction, heart failure and even death without timely treatment [1, 2]. Cardiac valve replacement is one of the most widely used strategies in the treatment of patients with severe VHD. In recent years, transcatheter valve implantation has shown great performance in VHD treatment with minimal invasiveness and a significantly shortened recovery period compared to that of conventional surgical valve replacement and thus has become a popular choice, especially for patients with surgical high-risk or aged patients [3–5]. Bioprosthetic heart valves (BHVs) made from porcine or bovine pericardia mainly consisting of collagen are often used in interventional VHD treatment, while most of the present BHVs are prepared via glutaraldehyde (Glut) crosslinking and suffer from calcification, thrombus, inflammation and endothelialization difficulty, which lead to limited durability (lifespan: 10–15 years) [6–11]. With the development of transcatheter valve replacement technology, it is extremely important to prepare BHVs with improved durability to improve the quality of life of VHD patients and make this technology more accessible to younger patients.

Glut could help to stabilize the main collagenic components of pericardial tissue by covalently linking the amino group of collagens and the aldehyde group of Glut [12, 13]. Nevertheless, residual Glut and aldehyde groups in BHVs are cytotoxic and would induce cell apoptosis, which leads to difficulties in endothelialization, and apoptotic cell debris provides potential nucleation sites for calcification [14–19]. Meanwhile, Glut-treated BHVs also induce the infiltration of immune cells and the secretion of immune factors, which are closely related to the occurrence and development of calcification [20, 21]. Moreover, the antithrombotic ability of Glut-crosslinked BHVs is insufficient, and the neoplasms on the surface of

BHVs triggered by blood clotting after valve replacement surgery will seriously affect the function of BHVs in vivo. Recent studies have shown that BHVs with anticoagulant properties would help to play their role after implantation [22, 23]. Although massive efforts, such as nonglutaraldehyde crosslinking agents, have been initiated to develop new alternatives to conventional Glut-treated BHVs, their clinical application performance still needs to be studied in detail. In addition, among these reported crosslinking agents, Glut-treated BHVs showed the best mechanical properties, which is crucial to the functioning of BHVs in vivo. Therefore, improving the durability of BHVs should endow BHVs with not only good biocompatibility and anti-calcification ability but also great anti-thrombus capacity.

In addition, prosthetic valve endocarditis (PVE) (incidence after transcatheter aortic valve replacement: approximately 3%) caused by bacterial invasion has also attracted attention in recent years due to its high fatality rate, while effective treatment strategies are still in urgent demand [24, 25]. To obtain ideal therapeutic effects, high doses and long-term antibiotic treatment are necessary, but they also cause severe side effects in patients [26, 27]. Thus, it would be very valuable to develop BHVs with antibacterial potential. However, conventional antibacterial materials tend to be cytotoxic and reduce cell adhesion. To address these problems, it would be meaningful to develop biocompatible BHVs with antibacterial ability, which is expected to prevent PVE in situ. Plant polyphenols, such as tannic acid (TA), have shown great oxidation resistance ability and interesting antibacterial ability with low cell toxicity [28–30]. In addition, TA has also been used as a crosslinking agent to fix pericardia, which has shown great structural stability and reduced calcification [31–35]. Therefore, TA is not only expected to endow BHVs with good antibacterial ability but also enhance its mechanical properties, which would be a potential candidate for the preparation of BHVs with improved durability.

Inspired by the antibacterial ability and crosslinking potential of TA, we prepared novel BHVs based on TA and polylysine to further improve the durability of Glut-crosslinked bovine pericardium (Glut-BP). Nanoaggregates made of TA and polylysine (Ply) could efficiently conjugate to Glut-BP via an aldol condensation reaction and Schiff base reaction between the remaining aldehyde groups of Glut-BP and the phenolic hydroxyl groups and amino groups of the nanoaggregates, respectively, as well as multiple hydrogen bonds to obtain functional BHVs (TPly-BP), which also enhanced the mechanical property, thermodynamic stability and resistance to collagenase degradation. TPly-BP showed good antibacterial properties, good hemocompatibility, reduced platelet adhesion, great cytocompatibility and improved endothelial cell adhesion compared to those of Glut-BP. Moreover, TPly-BP also showed great anti-calcification ability in vivo with reduced inflammation. Therefore, TPly-BP would be a potential candidate for BHVs.

2 Materials and methods

2.1 Material

Tannic acid (TA), polylysine (M*w* 5000), trihydroxymethyl aminomethane (Tris), and 50% Glut solution were purchased from Shanghai Titan Scientific Co., Ltd. (Shanghai, China). Type I collagenase was obtained from BioFroxx. Bovine pericardia (BPs) were purchased from a slaughter house (cattles, 10 pericardia from different cattles, and the age of the scalpers was approximately 2.5 years old). All chemicals and materials were used without further purification.

2.2 Modification of TPly-BP

First, fresh BPs (10 pieces) were treated with 0.5% SDS (mass/volume) at 4 °C for 24 h with continuous shaking, washed with saline (4 °C) five times (shaking for 5 min each time), and crosslinked by 1% Glut (mass/volume) for 48 h to obtain Glut-BP. Subsequently, TA was dissolved in 30 mM Tris buffer (pH = 8.5) to prepare a 3 mg/mL TA solution, and polylysine equal in weight to TA was added to prepare a TPly nanoaggregate suspension. Glut-BP was immersed in the above suspension shaking at room temperature (80 rpm) for 24 h. TPly nanoaggregate-modified BPs (TPly-BP) were obtained by rinsing with saline with continuous shaking for 30 min (n = 3). The solution was replaced with fresh saline every 10 min. TA-BP was also prepared in the same method without adding polylysine (n = 3).

2.3 Characterization

All experiments were performed at least three times unless otherwise noted. Representative data are presented. Glut-BP, TA-BP and TPly-BP were cut into small pieces of different sizes, and these pieces were randomly selected to study their physicochemical properties and biological functions. Glut-BP, TA-BP and TPly-BP were cut into square patches (8 × 8 mm) and lyophilized, and the micromorphology of the fibrous structure and morphology were observed by scanning electron microscopy (SEM, Thermo Scientific Apreo 2 C). The chemical components of the sample surfaces were characterized by an attenuated total reflection Fourier transformed infrared spectrometer (ATR-FTIR, Frontier) and X-ray photoelectron spectroscopy (Escalab 250Xi, Thermo Fisher Scientific Inc., USA). The thermal shrinkage temperature was measured by a differential scanning calorimeter (DSC204F01) with a temperature interval ranging

from 40 to 120 °C. The water contact angle was measured by an OCA20 (Dataphysis, Germany). The mechanical properties of the samples were tested by a universal tensile machine (AI-7000 S) with a loading speed of 20 mm/min. These pericardia were cut into small pieces of different sizes, and these pieces were randomly selected to study their biological functions.

2.4 Enzymatic degradation resistance test

Lyophilized samples were cut into square patches (10 × 10 mm, n = 4), and the initial weight W_0 of each sample was recorded. The samples were incubated in 1 mL PBS containing 1 mg/mL type I collagenase (125 U/mL) and incubated at 37 °C in a shaking incubator for 24 h. Then, the samples were washed three times with deionized water after processing, the water was completely removed, and the samples were weighed again (W_1). The weight loss ratio of each sample was calculated with the following formula:

$$\text{Weight loss ratio} = \frac{W_0 - W_1}{W_0} \times 100\%$$

2.5 In vitro antibacterial assays

Tetracycline-resistant Escherichia coli (TREC) and methicillin-resistant Staphylococcus aureus (MRSA) were selected to study the ability of pericardia to resist drug-resistant bacteria.

2.5.1 Bacterial anti-adhesion test

Anti-adhesion ability was tested according to our previous works [28, 36, 37]. In brief, biological valve samples (10 × 10 mm, n = 3) were incubated with 1 mL of bacterial suspension (10^7 CFU mL^{-1}) in a 24-well plate at 37 °C for 2 h. Afterward, the samples were rinsed three times with normal saline, and the bacteria strongly adhered to the surface were dispersed in 5 mL of sterile normal saline by an ultrasonic cleaner. Finally, 20 μL of the above suspension was coated on a nutrient agar plate, and the colony-forming units were counted after further culturing at 37 °C for 18 h. Additionally, bacteria adhered to the BP fibers were further observed by SEM. The samples that were washed with normal saline three times to remove the unadhered bacteria were fixed in Glut (2.5 vol%) for 4 h at 4 °C and dehydrated with a series of ethanol solutions (25%, 50%, 75%, 95%, 100%). Finally, the dried biological BPs were investigated by SEM.

2.5.2 Bactericidal activity

Briefly, 500 mg of the sample cut into small pieces was put into a conical flask coated with 10 mL of bacterial suspension at a concentration of 5×10^5 CFU/mL. The flask was shaken (120 rpm) at 37 °C. After 0 and 4 h of incubation, 20 μL of bacterial suspension was coated on a nutrient agar plate. The colony-forming units were counted after culturing at 37 °C for 18 h. Moreover, the above bacterial suspension collected was stained to visualize under a fluorescence microscope with a cover slip.

2.6 Platelet adhesion

Fresh rabbit blood was centrifuged at 1500 rpm for 15 min to obtain the upper platelet-rich plasma (PRP). Glut-BP, TA-BP and TPly-BP with a diameter of 6 mm (n = 3) were seeded on 96-well plates and washed with PBS three times. Afterwards, 100 μL of PRP was added, and the plate was incubated at 37 ℃ for 2 h. The BPs were washed with PBS three times and fixed with 2.5% Glut for 2 h, followed by washing with PBS three times. Then, the BPs were treated with gradient dehydration of ethanol/water solution and freeze drying. The adhered HUVECs were observed by scanning electron microscopy (Thermo Scientific Apreo 2 C).

2.7 Determination of the hemolysis ratio

Fresh rabbit blood (2 mL) was centrifuged at 1500 rpm for 15 min, and the red blood cell (RBC) layer was collected and diluted with 40 mL 0.9% NaCl solution. Glut-BP, TA-BP and TPly-BP (diameter of 1 cm) (n = 4) were placed in a 24-well plate with 2 mL RBC diluent, and the plate was incubated at 37 ℃ for 1 h. RBC diluent without BPs was used as the negative control, and RBC diluent containing 0.2% Triton X-100 was used as the positive control. After incubation, the RBC suspension was centrifuged at 3000 rpm for 15 min. The resulting solution was photographed, and the absorption at 540 nm was detected with a microplate reader (Varioskan Flash, Thermo Fisher Scientific, USA).

$$\text{Hemolysis ratio} = \frac{OD_{BP} - OD_{negative}}{OD_{positive} - OD_{negative}} \times 100\%$$

2.8 In vitro cytotoxicity evaluation

The cytotoxicity of Glut-BP, TA-BP and TPly-BP was evaluated according to ISO 10993-5 testing standards for implantable medical devices with modification. TPly nanoaggregates were utilized to eliminate the remaining aldehyde groups of glutaraldehyde to improve the biocompatibility of BP; therefore, TA-BP and TPly-BP could not be sterilized via Glut solution. Accordingly, pieces of Glut-BP, TA-BP and TPly-BP sterilized by ultraviolet irradiation (1 × 1 cm, n = 5) were incubated with 1 mL of DMEM (suspended with 1% penicillin–streptomycin and 5% fetal bovine serum) at 37 °C in a 5% CO_2 atmosphere for 3 days.

Human umbilical vein endothelial cells (HUVECs) were seeded in 96-well plates at a density of 5,000 cells per well and incubated for 24 h. Then, extracts of Glut-BP, TA-BP and TPly-BP were added, and the cells were incubated for another 24 h. Finally, the relative cell viability was measured by CCK8 assay according to the kit instruction manual.

2.9 Endothelial cell adhesion experiment

Glut-BP, TA-BP and TPly-BP round pieces with a diameter of 1 cm sterilized by ultraviolet irradiation (n = 3) were put into 48-well plates, and HUVEC suspensions with 15,000 cells were added to each well. After incubation in a humidified atmosphere with 5% CO_2 at 37 ℃ for 36 h, the relative cell amount on these BPs was detected by a CCK8 kit. The living cells on the surface of BPs were stained with Calcein AM and imaged via fluorescence microscopy (Olympus). Moreover, cells on the surface of BPs were also stained with TRITC-phalloidin (red) and DAPI (blue) after fixation with Glut (2.5%) for 30 min. The morphology of HUVECs was observed by laser confocal microscopy (Leica Stellaris 5).

2.10 Subcutaneous implantation

Glut-BP, TA-BP and TPly-BP (diameter of 1 cm) were sterilized by ultraviolet irradiation (for each group, n = 8) and immersed in sterile PBS. Male Sprague Dawley (SD) rats (three weeks, approximately 50 g) were anesthetized by pentobarbital solution (at dosage of 3 mL/kg) via intraperitoneal injection. Longitudinal surgical incisions were made on the midline of the SD rats' back, and BPs were implanted into subcutaneous pockets on both sides of the incision (two samples per rat). SD rats were sacrificed after two months, and the BPs were isolated together with the fibrous capsule to perform histological analysis and immunohistochemical staining. Alizarin red and von Kossa staining were used to stain calcium deposits. CD68 antibody (Servicebio, diluted at 1:100 in PBST buffer containing 1% BSA) was utilized to label macrophagocytes, and the specimens were then incubated with HRP-conjugated goat anti-rabbit IgG (Servicebio, diluted at 1:200) for 2 h at 25 °C. Afterwards, the sections were treated with a DAB kit (Servicebio) and then hematoxylin (Solarbio). Some of the BPs were separated from the fibrous capsule, lyophilized and weighed. After digestion with 6 M HCl, the calcium content was measured by ICP–OES (PE Avio 200).

2.11 Quantification and statistical analysis

Independent tests were carried out at least three times. Prism (GraphPad 8) was used for data plotting. Unless otherwise specified, the data are presented as the mean ± standard deviation (SD). For comparison of multiple samples, statistical significance was performed by one-way ANOVA and Bonferroni's multiple comparisons test. For pairwise comparisons, a two-tailed Student's t test was used for statistical significance analysis. A p value less than 0.05 was considered to be statistically significant. $^{*}p < 0.05$, $^{**}p < 0.01$, $^{***}p < 0.001$, $^{****}p < 0.0001$. n.s., not significant.

3 Results and discussions

3.1 Preparation and characterization of TPly-BP

Fresh pericardia were decellularized vis SDS treatment, which was confirmed by H&E images in Additional file 1: Fig. S1. Then the decellularized pericardia were crosslinked by Glut. In this work, TA was selected as an antibacterial polyphenol to react with biocompatible Ply to form hybrid nanoaggregates (TPly) under weakly alkaline conditions via multiple hydrogen bonds and covalent bonds between TA and Ply since the phenolic hydroxyl groups of TA gradually oxidize to quinone groups under alkaline conditions, which react with the amino groups of Ply through a Schiff base reaction [38, 39]. Then, due to the multiple active pyrogallol groups, the formed TPly nanoaggregates were used to modify Glut-BP, in which pyrogallol groups were supposed to react with collagen fibers through Schiff base coupling, Michael addition reactions, and hydrogen-bond interactions (illustration in Scheme 1 of TPly-BP) [33, 34]. In this work, TA-modified Glut-BP was also carried out via a similar cross-linking mechanism, and the obtained TA-BP sample was used as a negative control sample in the following studies. After modification, the morphologies of Glut-BP, TA-BP, and TPly-BP samples were investigated by SEM. As shown in Fig. 1A, the compactness of the collagen structure of the TA-BP or TPly-BP samples was higher than that of the Glut-BP sample, indicating the enhanced cross-linking effect of TA or hybrid TPly molecules with collagen, which was similar to previous work [32, 34]. In addition, deposited nanoaggregates can be clearly observed on collagen fibers of the TPly-BP sample, confirming the supramolecular self-assembly of tannic acids and polylysine polymer. In addition, compared with the Glut-BP sample (83° ± 4.4°), the surface hydrophilicity of TA-BP and TPly-BP samples was increased with water contact angle values of 65.6° ± 2.1° and 58.8° ± 1.2° (Additional file 1: Fig. S2), respectively, which was attributed to the introduction of hydrophilic TA molecules. Moreover, the chemical component changes on the valve surface after the introduction of TA or TPly nanoaggregates were also confirmed by ATR-FTIR (Fig. 1B). The absorption band at 1725 cm^{-1} appeared in the spectra of TA-BP and TPly-BP owing to the stretching vibration of the C = O groups of quinonyl. Stretching vibrations for C–O (esters, ethers)

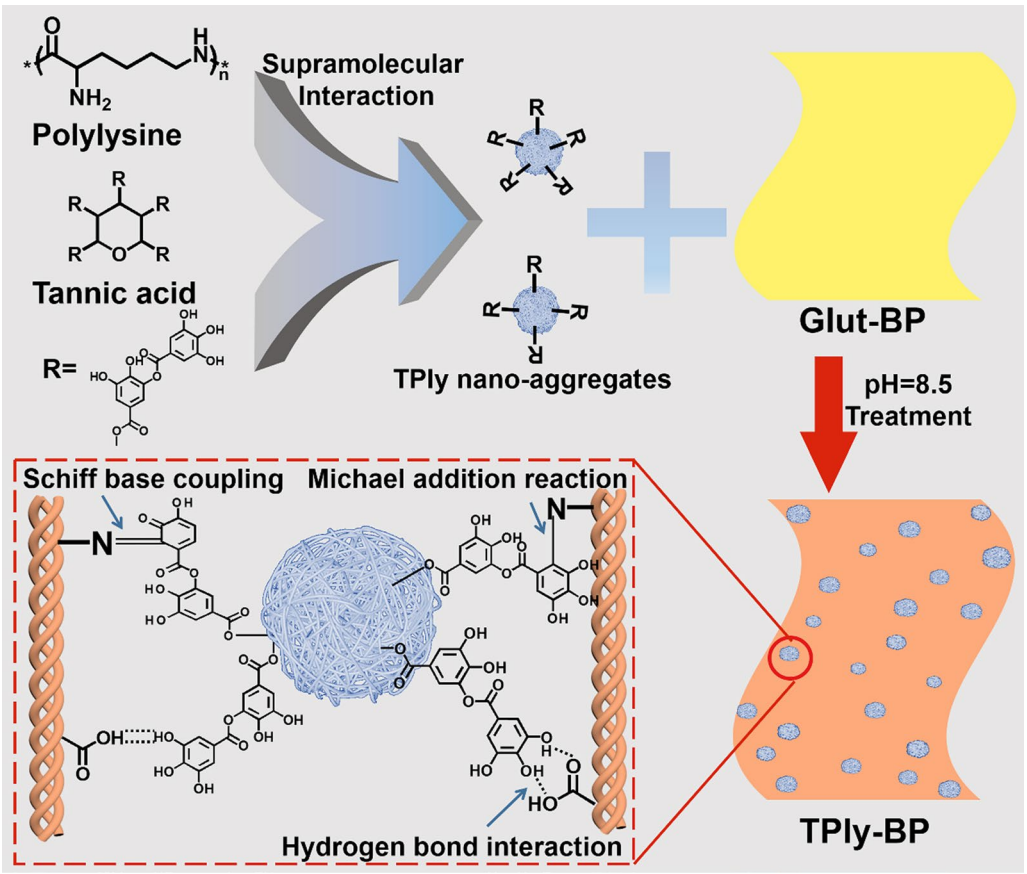

Scheme 1 Schematic illustration of the modification of BPs by hybrid TPly nanoaggregates

at 1200 cm^{-1} were also visible, suggesting the successful introduction of TA or TPly nanoaggregates to BPs.

Furthermore, the cross-linking mechanism of TPly nanoaggregates was verified by XPS analysis. As shown in Fig. 1C, signals of C1 s, N1 s, and O1 s, which are characteristic peaks of collagen fibers, were detected for all three samples. However, the O1 s peak intensity of the TPly-BP sample was higher than that of the Glut-BP and TA-BP samples (see results summarized in Table 1) due to the TPly nanoaggregates introduced onto collagen fibers. Then, the high-resolution spectra of the N1 s peaks of the three samples were carefully analyzed and are displayed in Fig. 1D. It is noted that, compared to the deconvolution N1 s spectra of the Glut-BP sample, two new peaks appeared at 400.0 and 400.5 eV for the TA-BP or TPly-BP sample, which can be assigned to the aromatic C = N bond from the Schiff base coupling and aromatic C − N bond from the Michael addition reaction. Moreover, the deconvolution of the N1 s XPS spectra of the TPly-BP sample also reveals an obvious C-NH_2 peak located at 401.3 eV, which is attributed to the cationic amino groups of polylysine. The above XPS results verify that the cross-linking mechanisms of TA and TPly nanoaggregates are both based on multiple reactions between pyrogallol groups and amino groups.

3.2 Enhanced thermodynamic stability and mechanical property of biological valve leaflets

The introduced cross-linking by TA or TPly nanoaggregates to Glut-BP is supposed to enhance the thermodynamic stability and mechanical property of biological valve leaflets. Therefore, a DSC instrument was first employed to investigate the thermostability of Glut-BP, TA-BP, and TPly-BP. The results in Fig. 2 A reveal that the TPly-BP sample exhibited the highest thermal denaturation temperature of 77.0 °C, which implied that the

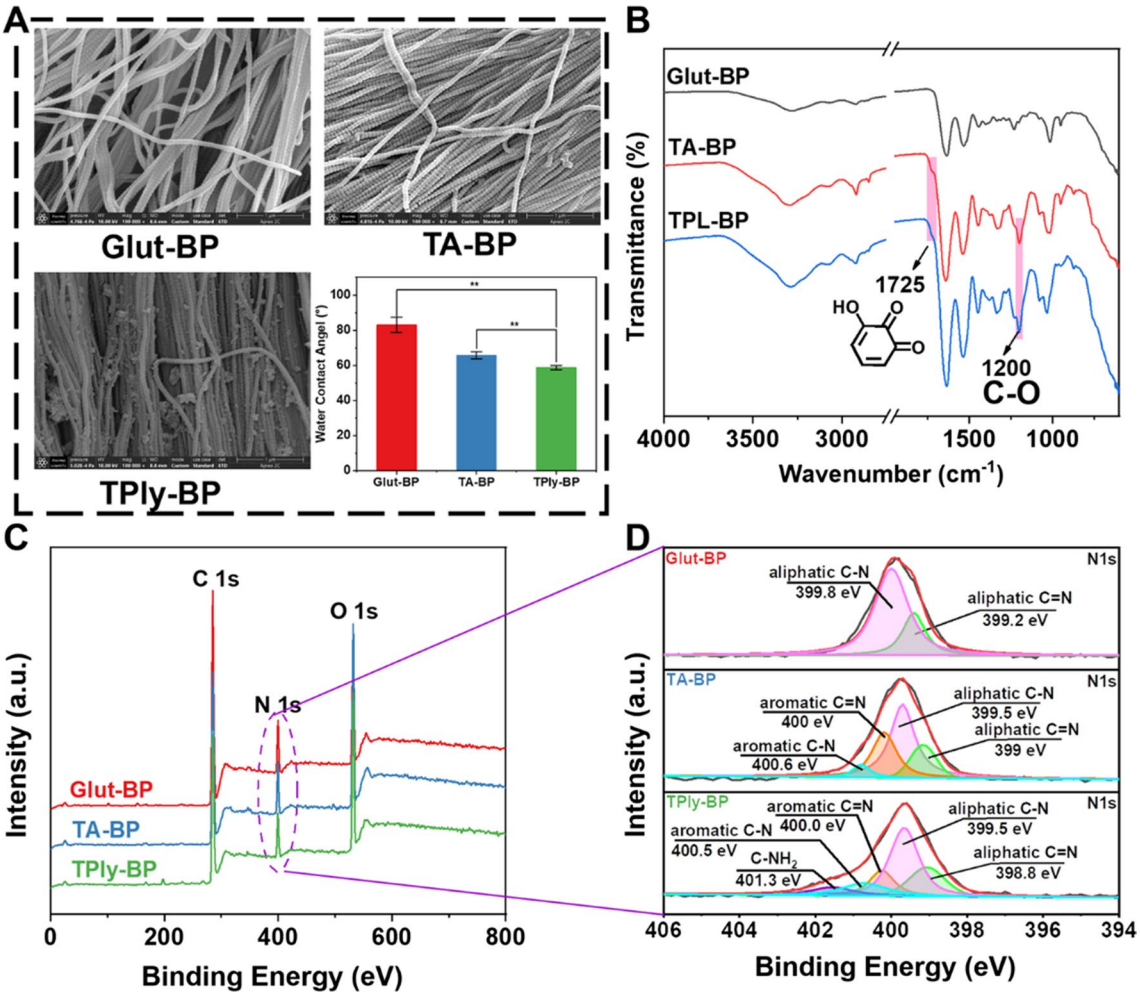

Fig. 1 Characterization of TPly-BP. **A** Typical SEM images, **B** ATR-FTIR and **C** wide scan XPS spectra of Glut-BP, TA-BP and TPly-BP. **D** High-resolution XPS spectra of N 1 s for Glut-BP, TA-BP and TPly-BP.

Table 1 Surface atom analysis determined by XPS spectra of three samples

Samples	C	N	O	C/O
Glut-BP	73.14	10.2	16.66	4.39
TA-BP	65.14	10.77	24.09	2.70
TPly-BP	63.38	11.32	25.3	2.51

hybrid TPly nanoaggregates could provide more cross-linking bonds with collagen fibers due to their nanosize and 3D spherical structure. In addition, the enzymatic degradation tests of the three samples in Fig. 2B also confirmed that the introduction of TPly nanoaggregates could enhance the stability of collagen, resulting in reduced weight loss of collagen, which was consistent with previous work. [32, 34, 35]

Good mechanical properties are necessary for valve material to be subjected to powerful blood flaw rushes and long openings and closures after implantation. Experimentally measured load–displacement curves are presented in Fig. 3 A for the samples. As important indicators for evaluating mechanical properties, ultimate tensile strength, extensibility and tangent modulus were selected for characterization (Fig. 3B and D). The ultimate tensile strength of TPly-BP (29.88 ± 2.44 MPa) was increased compared with that of Glut-BP (13.97 ± 1.77 MPa). The extensibility of the TPly-BP samples increased slightly, indicating that the modified samples would not reduce compliance and mechanical fatigue

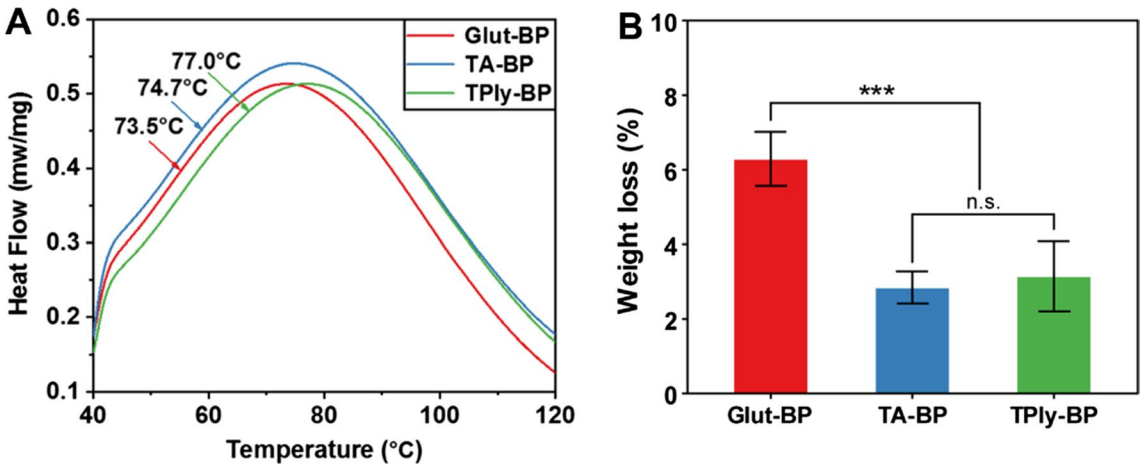

Fig. 2 Thermodynamic stability. **A** DSC plots for Glut-BP, TA-BP and TPly-BP. **B** Weight loss ratio of Glut-BP, TA-BP and TPly-BP after enzymatic degradation (n = 4)

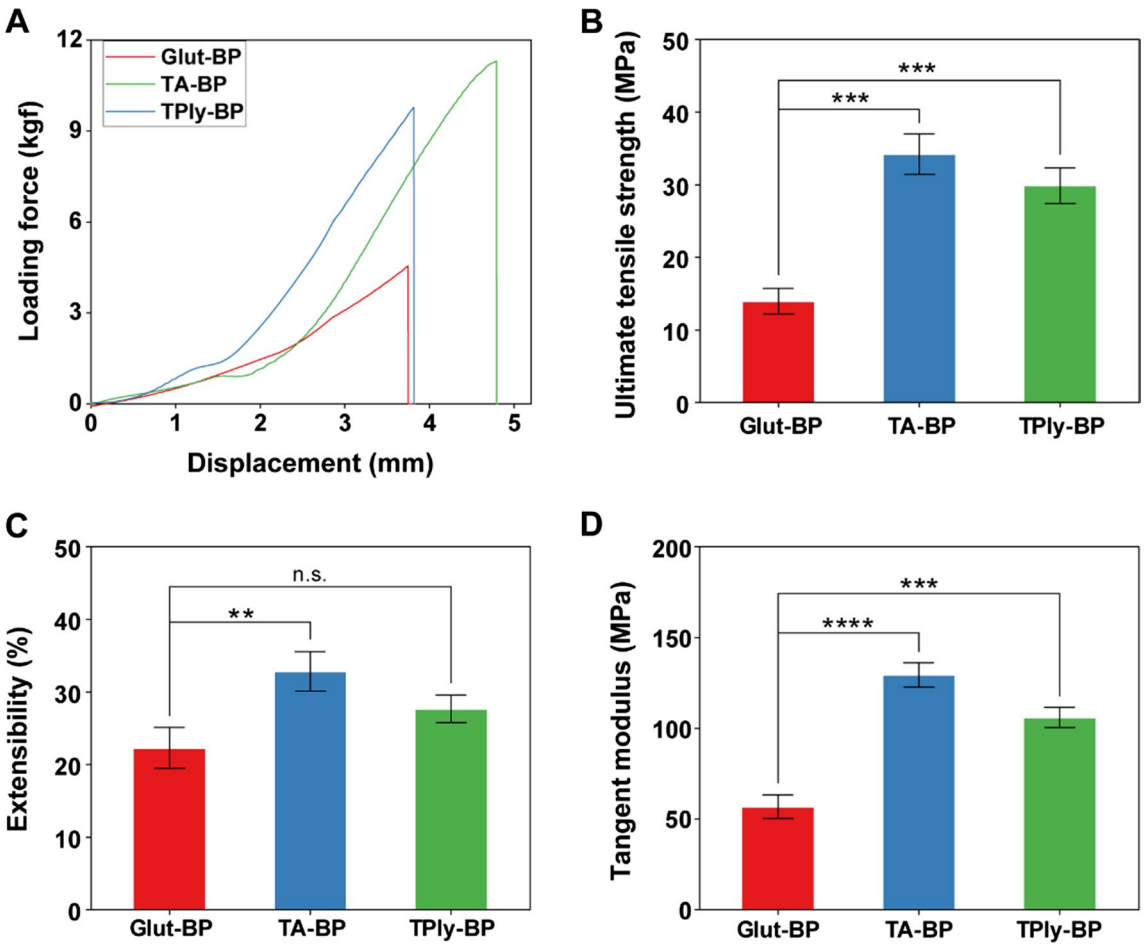

Fig. 3 Mechanical properties of TPly-BP. **A** Tensile displacement and load curves, **B** ultimate tensile strength, **C** extensibility and **D** tangent modulus of Glut-BP, TA-BP and TPly-BP.

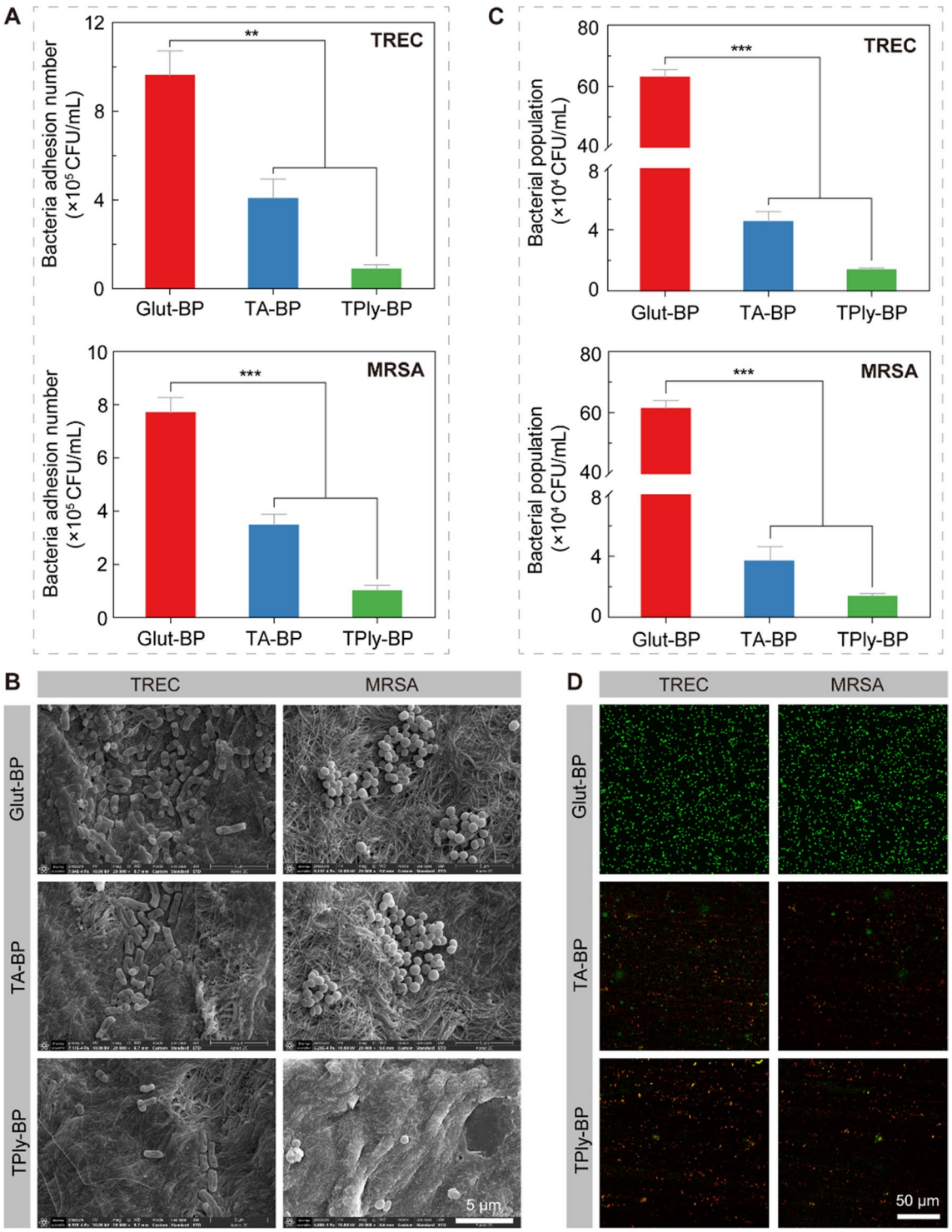

Fig. 4 Antibacterial activity of Glut-BP, TA-BP and TPly-BP. **A** The number of adhered bacteria on the surface of Glut-BP, TA-BP and TPly-BP. **B** The morphologies of bacterial adhesion on the valve surface by SEM (20,000×). Scale bar, 5 μm. **C** Bacterial population and **D** CLSM images of bacteria after culturing for 4 h with Glut-BP, TA-BP and TPly-BP.

resistance. In addition, the TPly-BP sample had a higher tangent modulus of 106.06 ± 5.54 MPa; nonetheless, that of the Glut-BP sample was only 56.82 ± 6.41 MPa. These results indicated that the introduction of TPly nanoaggregates could serve as a kind of cross-linking agent, which would not reduce the mechanical properties of Glut-BP.

3.3 Antibacterial property of TPly-BP

Drug-resistant bacterial infection is one of the important causes of postoperative complications in clinical valve implants. An important factor in antibacterial properties is the ability to resist bacterial adhesion. Therefore, the bacterial ant-adhesion capacity against tetracycline-resistant Escherichia coli (TREC) and methicillin-resistant Staphylococcus aureus (MRSA) of biological valves was first measured. Compared with the Glut-BP group, the number of bacteria adhered on TA-BP and TPly-BP dropped significantly (Fig. 4A), which is a clear indication of the bacterial antiadhesion activity of the modification valve material. However, by SEM observation of bacteria adhered on the sample surface (Fig. 4B), there were still several dead bacteria adhered on the TA-BP surface, while more bacteria were rinsed down from the surface of TPly-BP due to the better hydrophilicity. We further tested the bactericidal activity of TPly-BP, as shown in Fig. 4C and D. Under the condition of high bacterial concentration, there were still some bacteria alive treated by TA-BP, but TPly-BP achieved a nearly 99% sterilization rate. This might be because dead bacteria easily adhere to the TA-BP surface, resulting in a decrease in bactericidal efficiency. These results prove that TPly-BP possesses excellent antibacterial ability enough to cope with postoperative bacterial infection.

3.4 Blood compatibility study

Good blood compatibility is essential for BHVs. The hemolysis ratio was studied via incubation with rabbit red blood cells, and the absorbance of the supernatant liquor at 540 nm was detected after centrifugation. As shown in Fig. 5A and Additional file 1: Fig. S3A, both TPly-BP and TA-BP showed less than a 0.5% hemolysis ratio, indicating their good blood compatibility. In addition, ideal BHVs should possess the ability to resist platelet adhesion to avoid the occurrence of thrombi. Glut-BP, TA-BP and TPly-BP were incubated with rabbit platelets, and the adhered platelets were observed by SEM. Obvious platelet adhesion with dendritic morphology could be observed on the surface of Glut-BP (Fig. 5C), while both TA-BP (Additional file 1: Fig. S3) and TPly-BP (Fig. 5C) showed much reduced platelet adhesion, which might be attributed to the blockage of the aldehyde group

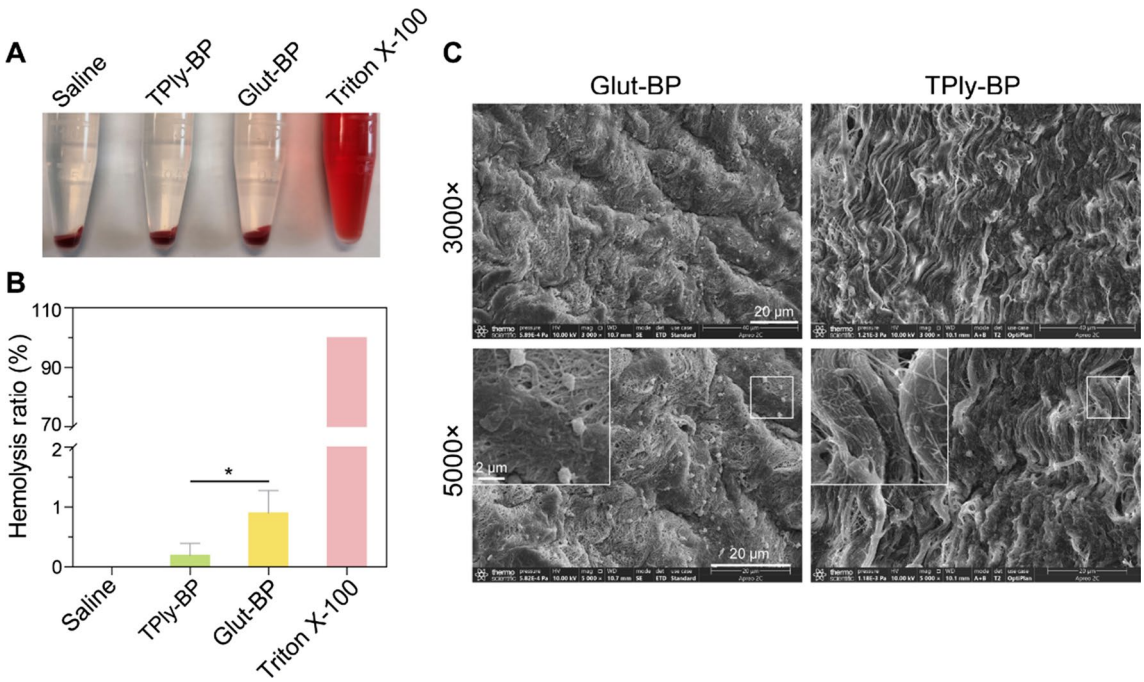

Fig. 5 Blood compatibility study of Glut-BP and TPly-BP. **A** Photograph of centrifuged red blood cell diluent after incubation with Glut-BP and TPly-BP at 37 °C for 1 h. **B** The hemolysis ratio of Glut-BP and TPly-BP (n = 4). **C** Representative SEM images of Glut-BP and TPly-BP at different magnifications (3000×, 5000×) after incubation with PRP for 2 h

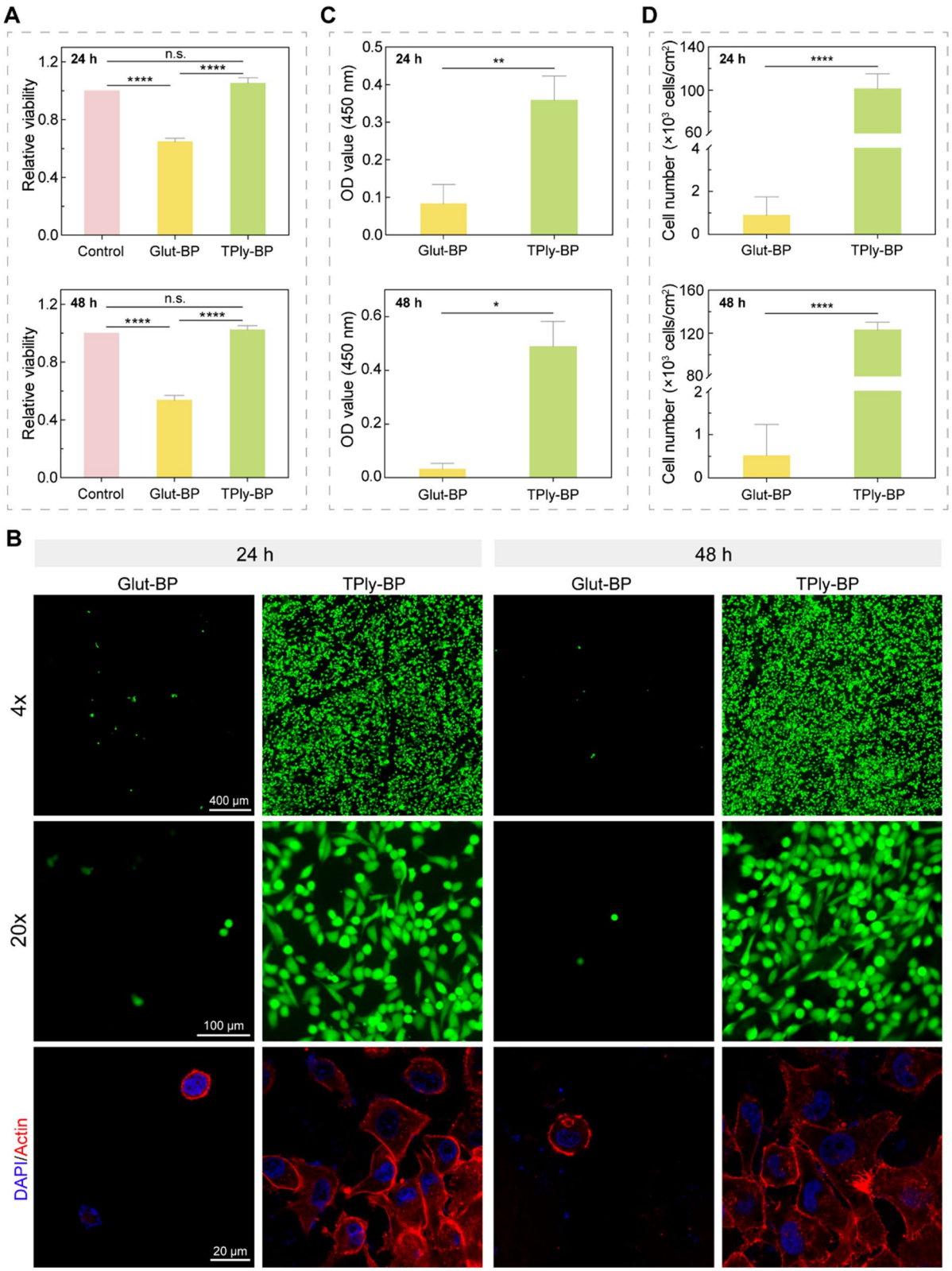

Fig. 6 The cytotoxicity of Glut-BP and TPly-BP. **A** Relative cell viability of HUVECs after incubation with the extracts of Glut-BP and TPly-BP for 24 and 48 h (n = 4). **B** Fluorescence images of HUVECs cultured on the surface of Glut-BP and TPly-BP stained with Calcein AM (green) and CLSM images of HUVECs cultured on the surface of Glut-BP and TPly-BP stained with TRITC-phalloidin (red) (actin) and DAPI (blue). **C** The OD value of HUVECs cultured on the surface of Glut-BP and TPly-BP (n = 3). **D** Cell number statistics of HUVECs cultured on the surface of Glut-BP and TPly-BP (n = 15)

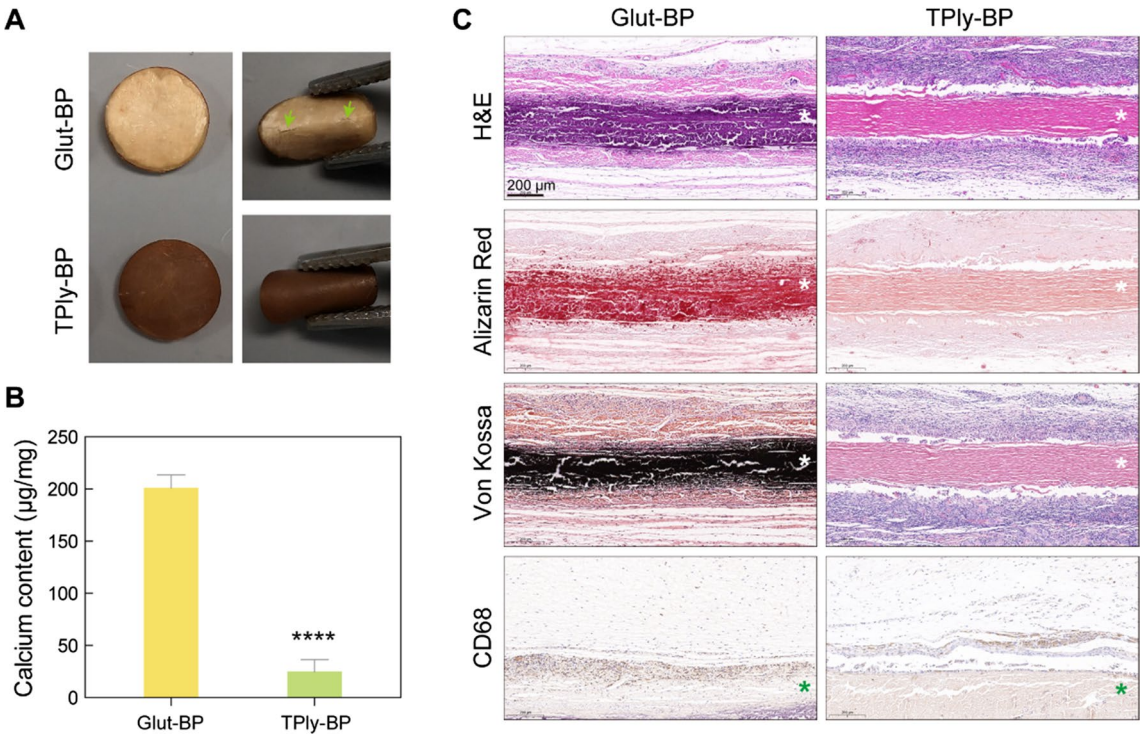

Fig. 7 Calcification of Glut-BP and TPly-BP after subcutaneous implantation in SD rats for 60 days. **A** Photographs of Glut-BP and TPly-BP removed from the SD rat. The green arrow indicates the crack of GA after half-folding. **B** Calcium contents of Glut-BP and TPly-BP removed from the SD rat determined by ICP–OES (n = 3). **C** Histological analysis of Glut-BP and TPly-BP removed from the SD rat. Calcium deposits were identified by Alizarin red and Von Kossa staining; H&E staining was used for histomorphological evaluation; immunohistochemical staining of CD68 was used to label macrophages (CD68-positive cells are marked brown). Scale bar, 200 μm

of Glut and the improved hydrophilicity, suggesting that TA-BP and TPly-BP would potentially reduce thrombi and prolong the lifespan of BHVs. These results indicate that TA-BP and TPly-BP have good blood compatibility.

3.5 Cytotoxicity of TPly-BP

The extracts of Glut-BP, TA-BP and TPly-BP were first prepared to study the potential cytotoxicity of these BPs. As shown in Fig. 6A, the extract of Glut-BP exhibited obvious cytotoxicity, with more than 40% of cells dying after incubation for 24 h, while the extract of TPly-BP showed good biocompatibility, and the relative cell viability was approximately 100% after incubation for both 24 and 48 h. However, the extract of TA-BP exhibited unsatisfactory cell viability, with less than 40% of cells surviving after incubation for 48 h (Additional file 1: Fig. S4). The strong cell inhibition ability of the TA-BP extract might be attributed to the dissociation of TA, which was adsorbed on the surface of BPs. Meanwhile, HUVECs were cultured on the surface of different BHVs previously placed in a 48-well plate. After incubation for 24 or 48 h, a CCK8 assay was utilized to study cell viability, and the cells were further stained with Calcein AM (green). As shown in Fig. 6B, obvious green fluorescence signals of cells were found in TPly-BP. However, Glut-BP and TA-BP (Fig. 6B and Additional file 1: Fig. S5) showed much less cell adhesion due to their poor biocompatibility. The CCK8 results in Fig. 6C and the cell number statistics result in Fig. 6D further confirmed the good biocompatibility and great endothelial cell affinity of TPly-BP. Moreover, the cytoskeleton and nucleus were stained with DAPI and TRITC-phalloidin, respectively, and observed by CLSM. The microfilaments of HUVECs could obviously be observed (Fig. 6B), which further confirmed the good biosecurity of TPly-BP.

3.6 In vivo anti-calcification study of TPly-BP

Anti-calcification is the key to improving the durability of BHVs. TA-BP might not be suitable for bioapplication due to its undesirable cytotoxicity. The anti-calcification ability of TPly-BP was evaluated via subcutaneous implantation in SD rats with Glut-BP as the control group. After implantation for 60 days, the rats were sacrificed, and the BPs were carefully isolated. As illustrated in Fig. 7A, obvious white hard plaque could be found in Glut-BP, which was fractured when the valve was folded in half with tweezers, suggesting the severe calcification of Glut-BP. In contrast, TPly-BP showed no obvious calcic plaque, with the color changing from yellowish brown to brown

due to the oxidation of the phenolic hydroxyl group. The calcium content of the BHVs was detected via ICP–OES after digestion. The calcium content of Glut-BP was up to 196 μg/mL (Fig. 7B), while TPly-BP showed a significantly reduced calcium content of approximately 30 μg/mL, indicating that TPly-BP was capable of reducing calcification. The histological staining results of H&E, Alizarin Red and Von Kossa in Fig. 7C further confirmed the severe calcification of Glut-BP. The calcification of Glut-BP might be attributed to its cytotoxicity and negative surface potential. The severe cytotoxicity of Glut-BP leads to cell death, and the inflammatory response results in potential structural destruction of BP. Meanwhile, the cell debris would serve as potential nucleation sites for calcification. In addition, the negative surface potential of GA-fixed pericardium would attract cations, such as calcium ions, which would exacerbate calcification. Interestingly, TPly-BP exhibited significantly reduced CD68 positive signals (brown) (Fig. 7C and Additional file 1: Fig. S6) compared to that of Glut-BP due to the strong oxidation resistance ability of TA; thus, TPly-BP would potentially reduce the inflammatory reaction of BHVs in vivo, which was beneficial to the long-lasting function of BHVs. All these results indicated that TPly-BP would be a potential candidate for BHVs.

4 Conclusion

In this work, we have prepared a novel BHVs TPly-BP based on natural TA and polylysine with good biocompatibility, good hemocompatibility, and great antibacterial and anti-calcification abilities. TPly nanoaggregate-modified BP could block the residual aldehyde group and further crosslink the BPs, resulting in an enhanced shrinkage temperature and improved structural stability and mechanical properties. Moreover, after 60 days of subcutaneous implantation, TPly-BP exhibited significantly reduced calcification compared to Glut-BP, indicating that TPly-BP would potentially improve the durability of BHVs. Together, these results suggest that TPly-BP would be a potential alternative to BHVs.

Supplementary Information

The online version contains supplementary material available at https://doi.org/10.1186/s42825-022-00105-3.

Additional file 1. Fig. S1. Images of H&E assays for fresh pericardium and SDS treated pericardium. **Fig. S2**. Water contact angle of Glut-BP, TA-BP and TPly-BP. **Fig. S3**. Blood compatibility study of Glut-BP and TA-BP. **Fig. S4**. Relative cell viability of HUVECs after incubation with the extracts of Glut-BP and TA-BP for 24 h and 48 h. **Fig. S5**. Fluorescence images of HUVECs cultured on the surface of Glut-BP and TA-BP stained by Calcein AM (green). **Fig. S6**. Immunohistochemical staining of CD68 (CD68 positives were marked brown).

Acknowledgements
We would be grateful to Jiayi Xu (Core Facilities of West China Hospital, Sichuan University) for taking laser scanning confocal images.

Authors' contributions
SL, SL and WZ conceived the idea and drafted the manuscript. ZC, JC and YD participated in part of the experiments. YD, YY, GL and MC analyzed the results and revised the manuscript. All authors read and approved the final manuscript.

Funding
This work was financially supported by the National Natural Science Foundation of China (81970325 and 82170375); Key Research and Development Support Project of Science & Technology Department of Chengdu (2021-YF08-00121-GX); Post-Doctor Research Project, West China Hospital, Sichuan University (Grant No. 20HXBH164 and 20HXBH105); Chinese Medical Association Cardiovascular Branch (CSC) Clinical Research Special Fund Project (CSCF2020B04); West China Hospital "1·3·5" Discipline of Excellence Project-"Percutaneous transcatheter aortic valve implantation" and "Mechanisms of aortic stenosis and the clinical applications" (ZYGD20002).

Availability of data and materials
All data from this study are presented in the paper and the additional file. The authors declare that the data in this article are reliable.

Declarations

Competing interests
The authors declare that they have no competing interests.

Ethics approval and consent to participate
All animal procedures were performed in accordance with the Guidelines for Care and Use of Laboratory Animals of West China Hospital, Sichuan University and approved by the Animal Ethics Committee of China (20220303074).

Author details
[1]Laboratory of Heart Valve Disease, West China Hospital, Sichuan University, 37 Guoxue Alley, Chengdu 610041, China. [2]The Key Laboratory of Leather Chemistry and Engineering of Ministry of Education, College of Biomass Science and Engineering, Sichuan University, Chengdu 610065, China. [3]University of California Davis, 1 Shields Ave, Davis, CA 95616, USA. [4]Faculty of Science and Engineering, Aachen-Maastricht Institute for Biobased Materials (AMIBM), Maastricht University, Brightlands Chemelot Campus, 6167 RD Geleen, The Netherlands. [5]Department of Cardiology, West China Hospital, Sichuan University, 37 Guoxue Alley, Chengdu 610041, China. [6]Regenerative Medicine Research Center, West China Hospital, Sichuan University, 37 Guoxue Alley, Chengdu 610041, China.

Received: 27 April 2022 Revised: 27 September 2022 Accepted: 13 October 2022
Published: 23 October 2022

References

1. Coffey S, Roberts-Thomson R, Brown A, Carapetis J, Chen M, Enriquez-Sarano M, Zuhlke L, Prendergast BD. Global epidemiology of valvular heart disease. Nat Rev Cardiol. 2021;18(12):853–64. https://doi.org/10.1038/s41569-021-00570-z.
2. Lindman BR, Clavel MA, Mathieu P, Iung B, Lancellotti P, Otto CM, Pibarot P. Calcific aortic stenosis. Nat Rev Dis Primers. 2016;2:16006. https://doi.org/10.1038/nrdp.2016.6.
3. Faroux L, Chen S, Muntane-Carol G, Regueiro A, Philippon F, Sondergaard L, Jorgensen TH, Lopez-Aguilera J, Kodali S, Leon M, Nazif T, Rodes-Cabau J. Clinical impact of conduction disturbances in transcatheter aortic valve replacement recipients: a systematic review and meta-analysis. Eur Heart J. 2020;41(29):2771–81. https://doi.org/10.1093/eurheartj/ehz924.
4. Faroux L, Guimaraes L, Wintzer-Wehekind J, Junquera L, Ferreira-Neto AN, del Val D, Muntané-Carol G, Mohammadi S, Paradis J-M, Rodés-Cabau J.

Coronary artery disease and transcatheter aortic valve replacement. J Am Coll Cardiol. 2019;74(3):362–72. https://doi.org/10.1016/j.jacc.2019.06.012.
5. Siontis GCM, Overtchouk P, Cahill TJ, Modine T, Prendergast B, Praz F, Pilgrim T, Petrinic T, Nikolakopoulou A, Salanti G, Sondergaard L, Verma S, Juni P, Windecker S. Transcatheter aortic valve implantation versus surgical aortic valve replacement for treatment of symptomatic severe aortic stenosis: an updated meta-analysis. Eur Heart J. 2019;40(38):3143–53. https://doi.org/10.1093/eurheartj/ehz275.
6. Arsalan M, Walther T. Durability of prostheses for transcatheter aortic valve implantation. Nat Rev Cardiol. 2016;13(6):360–7. https://doi.org/10.1038/nrcardio.2016.43.
7. VeDepo MC, Detamore MS, Hopkins RA, Converse GL. Recellularization of decellularized heart valves: progress toward the tissue-engineered heart valve. J Tissue Eng. 2017. https://doi.org/10.1177/2041731417726327.
8. Fatima B, Mohananey D, Khan FW, Jobanputra Y, Tummala R, Banerjee K, Krishnaswamy A, Mick S, Tuzcu EM, Blackstone E, Svensson L, Kapadia S. Durability data for bioprosthetic surgical aortic valve: a systematic review. JAMA Cardiol. 2019;4(1):71–80. https://doi.org/10.1001/jamacardio.2018.4045.
9. Costa G, Criscione E, Todaro D, Tamburino C, Barbanti M. Long-term transcatheter aortic valve durability. Interv Cardiol. 2019;14(2):62–9. https://doi.org/10.15420/icr.2019.4.2.
10. Nitsche C, Kammerlander AA, Knechtelsdorfer K, Kraiger JA, Goliasch G, Dona C, Schachner L, Ozturk B, Binder C, Duca F, Aschauer S, Zimpfer D, Bonderman D, Hengstenberg C, Mascherbauer J. Determinants of bioprosthetic aortic valve degeneration. JACC Cardiovasc Imaging. 2020;13(2 Pt 1):345–53. https://doi.org/10.1016/j.jcmg.2019.01.027.
11. Yu T, Yang W, Zhuang W, Tian Y, Kong Q, Chen X, Li G, Wang Y. A bioprosthetic heart valve cross-linked by a nonglutaraldehyde reagent with improved biocompatibility, endothelialization, anti-coagulation and anti-calcification properties. J Mater Chem B. 2021;9(19):4031–8. https://doi.org/10.1039/d1tb00409c.
12. Mathapati S, Bishi DK, Guhathakurta S, Cherian KM, Venugopal JR, Ramakrishna S, Verma RS. Biomimetic acellular detoxified glutaraldehyde cross-linked bovine pericardium for tissue engineering. Mater Sci Eng C Mater Biol Appl. 2013;33(3):1561–72. https://doi.org/10.1016/j.msec.2012.12.062.
13. Grabenwöger M, Sider J, Fitzal F, Zelenka C, Windberger U, Grimm M, Moritz A, Böck P, Wolner E. Impact of glutaraldehyde on calcification of pericardial bioprosthetic heart valve material. Ann Thorac Surg. 1996;62(3):772–7. https://doi.org/10.1016/s0003-4975(96)00442-0.
14. Umashankar PR, Mohanan PV, Kumari TV. Glutaraldehyde treatment elicits toxic response compared to decellularization in bovine pericardium. Toxicol Int. 2012;19(1):51–8. https://doi.org/10.4103/0971-6580.94513.
15. Lee C, Kim SH, Choi SH, Kim YJ. High-concentration glutaraldehyde fixation of bovine pericardium in organic solvent and postfixation glycine treatment: in vitro material assessment and in vivo anticalcification effect. Eur J Cardiothorac Surg. 2011;39(3):381–7. https://doi.org/10.1016/j.ejcts.2010.07.015.
16. Manji RA, Lee W, Cooper DKC. Xenograft bioprosthetic heart valves: past, present and future. Int J Surg. 2015;23:280–4. https://doi.org/10.1016/j.ijsu.2015.07.009.
17. Rodriguez-Gabella T, Voisine P, Puri R, Pibarot P, Rodes-Cabau J. Aortic bioprosthetic valve durability: incidence, mechanisms, predictors, and management of surgical and transcatheter valve degeneration. J Am Coll Cardiol. 2017;70(8):1013–28. https://doi.org/10.1016/j.jacc.2017.07.715.
18. Lim HG, Kim SH, Choi SY, Kim YJ. Anticalcification effects of decellularization, solvent, and detoxification treatment for genipin and glutaraldehyde fixation of bovine pericardium. Eur J Cardiothorac Surg. 2012;41(2):383–90. https://doi.org/10.1016/j.ejcts.2011.05.016.
19. Tod TJ, Dove JS. The association of bound aldehyde content with bioprosthetic tissue calcification. J Mater Sci Mater Med. 2016;27(1):8. https://doi.org/10.1007/s10856-015-5623-z.
20. Yu T, Chen X, Zhuang W, Tian Y, Liang Z, Kong Q, Hu C, Li G, Wang Y. Nonglutaraldehyde treated porcine pericardium with good biocompatibility, reduced calcification and improved Anti-coagulation for bioprosthetic heart valve applications. Chem Eng J. 2021;414:128900. https://doi.org/10.1016/j.cej.2021.128900.
21. Northeast R, Constable M, Burton HE, Lawless BM, Gramigna V, Lim Goh K, Buchan KG, Espino DM. Mechanical testing of glutaraldehyde cross-linked mitral valves. Part one: in vitro mechanical behavior. Proc Inst Mech Eng H. 2021;235(3):281–90. https://doi.org/10.1177/0954411920975894.
22. Wang Y, Ma B, Liu K, Luo R, Wang Y. A multi-in-one strategy with glucose-triggered long-term antithrombogenicity and sequentially enhanced endothelialization for biological valve leaflets. Biomaterials. 2021;275:120981. https://doi.org/10.1016/j.biomaterials.2021.120981.
23. Liu K, Li M, Zhang F, Wang Y, Chen C, Wei Y, Yang L, Luo R, Wang Y. Chemical bonding of biological valve leaflets with an aminated zwitterionic copolymer for long-term anticoagulation and improved anti-calcification. Chem Eng J. 2021;426:131803. https://doi.org/10.1016/j.cej.2021.131803.
24. Alexis SL, Malik AH, George I, Hahn RT, Khalique OK, Seetharam K, Bhatt DL, Tang GHL. Infective endocarditis after surgical and transcatheter aortic valve replacement: a state of the art review. J Am Heart Assoc. 2020;9(16):e017347. https://doi.org/10.1161/JAHA.120.017347.
25. Butt JH, Ihlemann N, De Backer O, Sondergaard L, Havers-Borgersen E, Gislason GH, Torp-Pedersen C, Kober L, Fosbol EL. Long-term risk of infective endocarditis after transcatheter aortic valve replacement. J Am Coll Cardiol. 2019;73(13):1646–55. https://doi.org/10.1016/j.jacc.2018.12.078.
26. Li S, Dong S, Xu W, Tu S, Yan L, Zhao C, Ding J, Chen X. Antibacterial hydrogels. Adv Sci. 2018;5(5):1700527. https://doi.org/10.1002/advs.201700527.
27. Ding X, Duan S, Ding X, Liu R, Xu F-J. Versatile antibacterial materials: an emerging arsenal for combatting bacterial pathogens. Adv Funct Mater. 2018;28(40):1802140. https://doi.org/10.1002/adfm.201802140.
28. Wang R, Yu R, Wang J, Xiang J, Chen C, Liu G, Liao X. Hierarchical collagen fibers complexed with tannic acid and Fe^{3+} as a heterogeneous catalyst for enhancing sulfate radical-based advanced oxidation process. Environ Sci Pollut Res Int. 2022. https://doi.org/10.1007/s11356-022-19907-3.
29. Ma W, Ding Y, Zhang M, Gao S, Li Y, Huang C, Fu G. Nature-inspired chemistry toward hierarchical superhydrophobic, antibacterial and biocompatible nanofibrous membranes for effective UV-shielding, self-cleaning and oil-water separation. J Hazard Mater. 2020;384:121476. https://doi.org/10.1016/j.jhazmat.2019.121476.
30. Zhang ZY, Sun Y, Zheng YD, He W, Yang YY, Xie YJ, Feng ZX, Qiao K. A biocompatible bacterial cellulose/tannic acid composite with antibacterial and anti-biofilm activities for biomedical applications. Mater Sci Eng C Mater Biol Appl. 2020;106:110249. https://doi.org/10.1016/j.msec.2019.110249.
31. Wang D, Jiang H, Li J, Zhou J, Hu S. Mitigated calcification of glutaraldehyde-fixed bovine pericardium by tannic acid in rats. Chin Med J (Engl). 2008;121(17):1675–9.
32. Cwalina B, Turek DA, Nozynski J, Jastrzebska M, Nawrat Z. Structural changes in pericardium tissue modified with tannic acid. Int J Artif Organs. 2005;28(6):648–53. https://doi.org/10.1177/039139880502800614.
33. Filova E, Stankova L, Eckhardt A, Svobodova J, Musilkova J, Pala J, Hadraba D, Brynda E, Konarik M, Pirk J, Bacakova L. Modification of human pericardium by chemical crosslinking. Physiol Res. 2020;69(1):49–59. https://doi.org/10.33549/physiolres.934335.
34. Jastrzebska M, Zalewska-Rejdak J, Wrzalik R, Kocot A, Mroz I, Barwinski B, Turek A, Cwalina B. Tannic acid-stabilized pericardium tissue: IR spectroscopy, atomic force microscopy, and dielectric spectroscopy investigations. J Biomed Mater Res A. 2006;78(1):148–56. https://doi.org/10.1002/jbm.a.30717.
35. Jin W, Guo G, Chen L, Lei Y, Wang Y. Elastin stabilization through polyphenol and ferric chloride combined treatment for the enhancement of bioprosthetic heart valve anticalcification. Artif Organs. 2018;42(11):1062–9. https://doi.org/10.1111/aor.13151.
36. Liu G, Xiang J, Xia Q, Li K, Yan H, Yu L. Fabrication of durably antibacterial cotton fabrics by robust and uniform immobilization of silver nanoparticles via mussel-inspired polydopamine/polyethyleneimine coating. Ind Eng Chem Res. 2020;59(20):9666–78. https://doi.org/10.1021/acs.iecr.9b07076.
37. Xiang J, Zhu R, Lang S, Yan H, Liu G, Peng B. Mussel-inspired immobilization of zwitterionic silver nanoparticles toward antibacterial cotton

gauze for promoting wound healing. Chem Eng J. 2021;409:128291. https://doi.org/10.1016/j.cej.2020.128291.
38. Liu G, Jiang Z, Chen C, Hou L, Gao B, Yang H, Wu H, Pan F, Zhang P, Cao X. Preparation of ultrathin, robust membranes through reactive layer-by-layer (LbL) assembly for pervaporation dehydration. J Membrane Sci. 2017;537:229–38. https://doi.org/10.1016/j.memsci.2017.05.025.
39. Zhong QZ, Richardson JJ, He A, Zheng T, Lafleur RPM, Li J, Qiu WZ, Furtado D, Pan S, Xu ZK, Wan LS, Caruso F. Engineered coatings via the assembly of amino-quinone networks. Angew Chem Int Ed Engl. 2021;60(5):2346–54. https://doi.org/10.1002/anie.202010931.

Publisher's Note